

# Mock LISA Data Challenge 1B: Improved Search for Galactic White Dwarf Binaries Using an $\mathcal{F}$ -Stat Template Bank

John T. Whelan<sup>1</sup>, Reinhard Prix<sup>2</sup>, and Deepak Khurana<sup>3</sup>

<sup>1</sup>Max-Planck-Institut für Gravitationsphysik (Albert-Einstein-Institut), Potsdam, Germany;

<sup>2</sup>Max-Planck-Institut für Gravitationsphysik (Albert-Einstein-Institut), Hannover, Germany;

<sup>3</sup>Indian Institute of Technology, Kharagpur, India

reinhard.prix@aei.mpg.de, john.whelan@aei.mpg.de



## Abstract

The  $\mathcal{F}$ -statistic is an optimal detection statistic for continuous gravitational waves, i.e. long-duration (quasi-) monochromatic signals with slowly-varying intrinsic frequency. This method was originally developed in the context of ground-based detectors, but can also be applied to LISA data. We report on the results of such a search on the Mock LISA Data Challenge 1B, and in particular the improvements in this search due to refinements of the search pipeline and the detector response.

## $\mathcal{F}$ -Statistic Method

A white-dwarf binary GW signal  $s(t)$  is characterized by its Doppler parameters  $\theta$ , i.e. frequency  $f$  and sky-position (ecliptic latitude  $\beta$ , longitude  $\lambda$ ), and its amplitude parameters  $\{\mathcal{A}^\mu\}_{\mu=1}^4 = \mathcal{A}^\mu(h_0, \cos i, \psi, \phi_0)$ , and can be written as

$$s(t; \mathcal{A}, \theta) = \mathcal{A}^\mu h_\mu(t; \theta). \quad (1)$$

Maximizing the likelihood ratio statistic over the four amplitude  $\mathcal{A}^\mu$ , results in maximum-likelihood estimators

$$\mathcal{A}_{\text{cand}}^\mu(x; \theta) = \mathcal{M}^{\mu\nu}(x \| h_\nu), \quad (2)$$

where  $\mathcal{M}^{\mu\nu}$  is the matrix inverse of  $\mathcal{M}_{\mu\nu} \equiv (h_\mu \| h_\nu)$ . Substituting the amplitude-estimator  $\mathcal{A}_{\text{cand}}^\mu$  into the likelihood ratio, we obtain the  $\mathcal{F}$ -statistic:

$$2\mathcal{F}(x; \theta) \equiv |\mathcal{A}_{\text{cand}}|^2 \equiv \mathcal{A}_{\text{cand}}^\mu \mathcal{M}_{\mu\nu} \mathcal{A}_{\text{cand}}^\nu, \quad (3)$$

and so we only need to search over the Doppler-space  $\theta = \{f, \beta, \lambda\}$ . If exactly targeting a signal, the expectation value of  $2\mathcal{F}$  is  $E[2\mathcal{F}(x; \theta_{\text{key}})] = 4 + |\mathcal{A}_{\text{key}}|^2$ .

## MLDC1B Pipeline

The LISA data stream will contain multiple strong signals, and we need to distinguish secondary maxima of  $2\mathcal{F}(x; \theta)$  in Doppler space (see Fig 1) from primary maxima belonging to weaker signals.

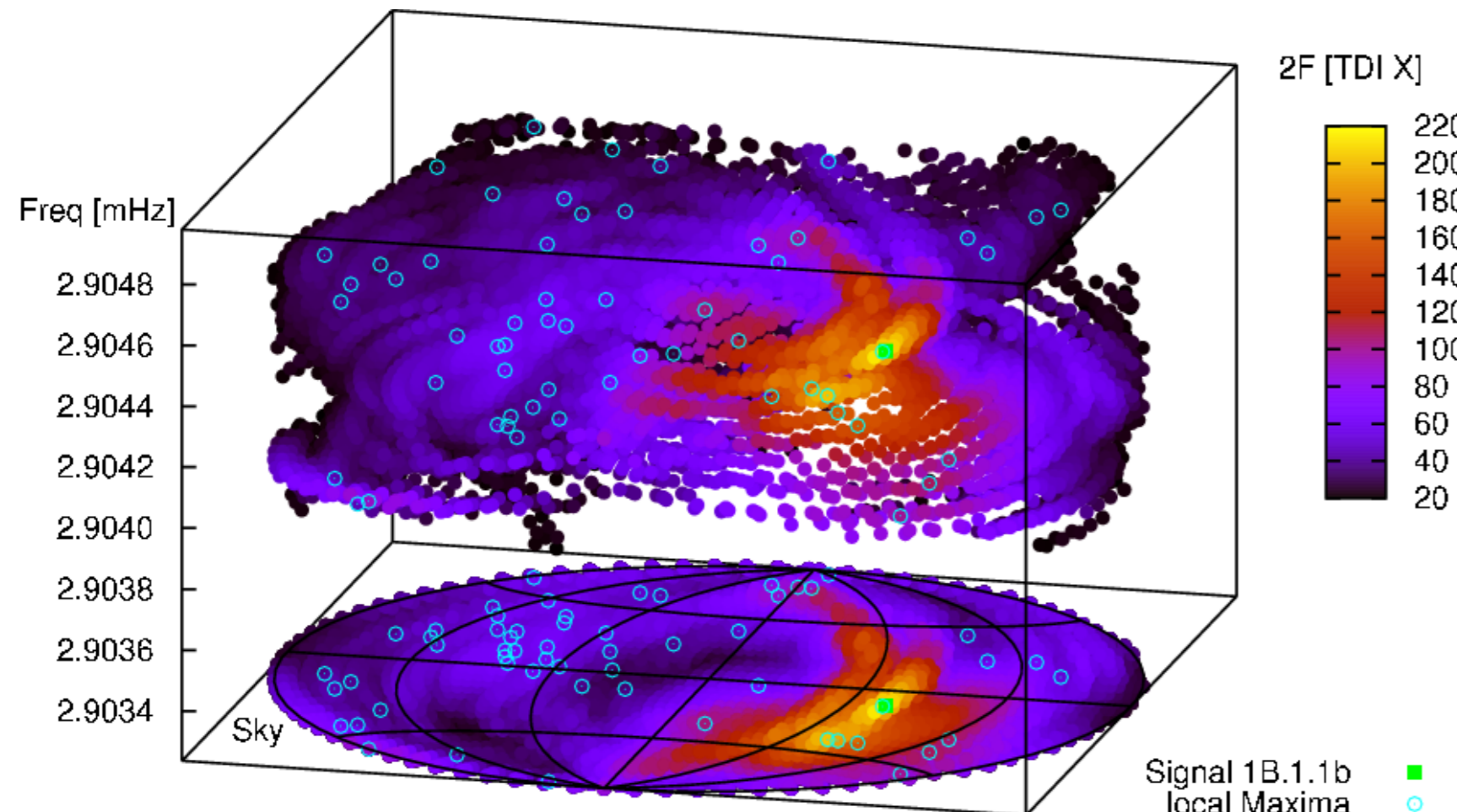


**Figure 1:** Doppler space structure for a single source (■) at  $f_s \sim 2.9044$  mHz. Shown are points with  $2\mathcal{F} > 20$  over the whole sky and within a Frequency window of  $f_s \pm 2 \times 10^{-4} f_s$ . Cyan circles indicate 3D local maxima in  $2\mathcal{F}$ .

Empirical observation shows that primary maxima show better coincidence in Doppler space between different TDI variables  $X, Y, Z$ , while secondary maxima can be vetoed by this method. Starting in MLDC2 [2], our pipeline (Fig. 2) makes use of a coincidence criterion based on the Doppler “distance”  $m$  between points separated by  $d\theta = \{df, d\beta, d\lambda\}$ , using the metric  $g_{ij}$ , namely

$$m = g_{ij} d\theta^i d\theta^j + \mathcal{O}(d\theta^3). \quad (4)$$

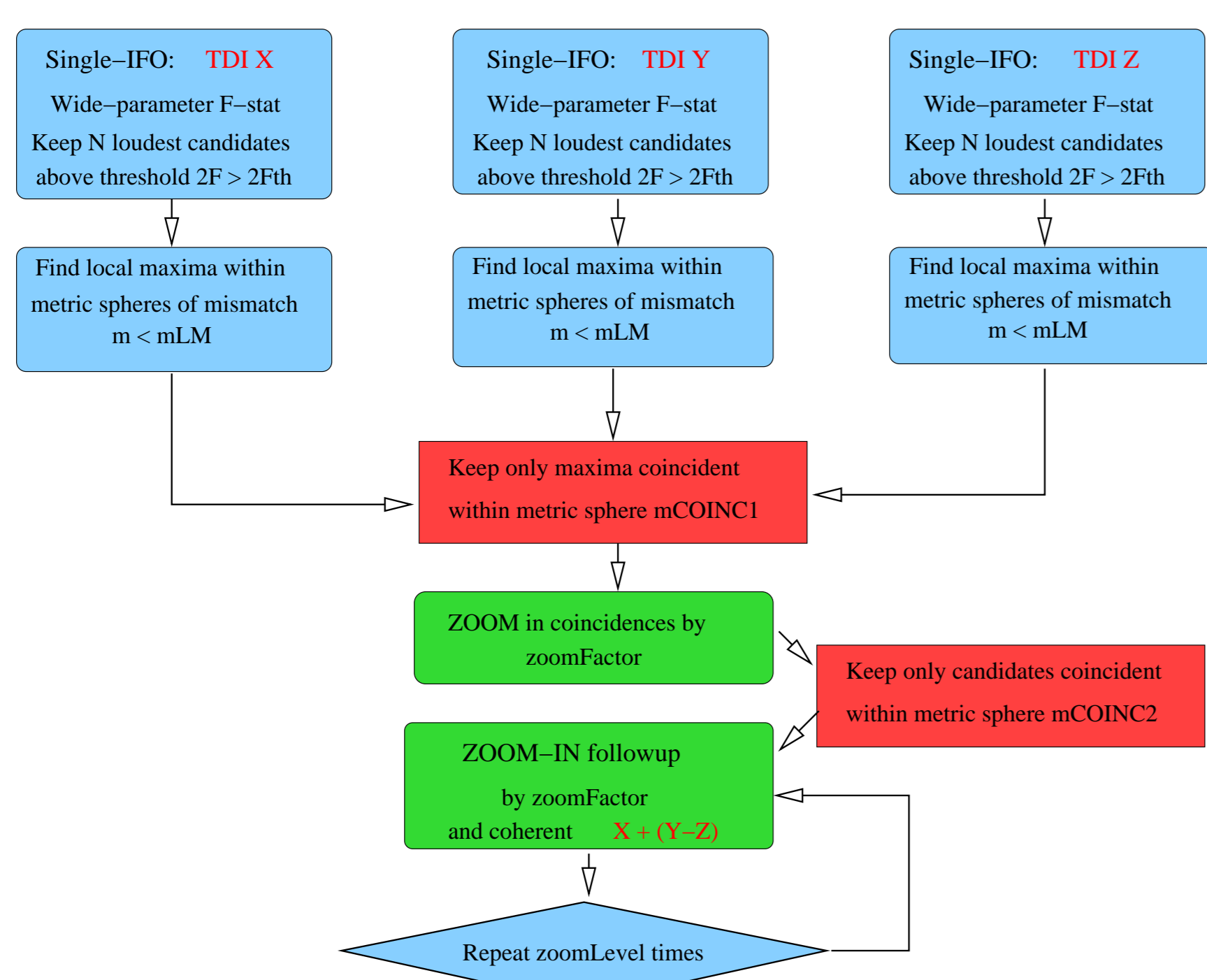


**Figure 2:** Pipeline used in MLDC1B. The final coincidence criterion used was  $m_{\text{COINC2}} \leq 0.35$ .

## Modelled TDI Response

In MLDC1+2 we used the long-wavelength limit (LWL) for converting LISA TDI observables to GW “strain”, e.g. for (LISA Simulator) TDI  $X$ :

$$\tilde{X}(f) \approx \left( \frac{ic}{4\pi fL} \right) \tilde{h}(f) \quad (5)$$

in terms of the usual interferometer strain

$$h \approx \frac{1}{2} (\hat{n}_2 \otimes \hat{n}_2 - \hat{n}_3 \otimes \hat{n}_3) : \vec{h} \quad (6)$$

where  $\hat{n}_2$  and  $\hat{n}_3$  are unit vectors along the LISA arms. Using the LWL in MLDC1+2, we recovered signals with accurate Doppler parameters, but inaccurate amplitude parameters  $\mathcal{A}^\mu$ .

A better approximation is the rigid adiabatic (RA) TDI response [4], i.e. for a signal from direction  $-\hat{k}$ :

$$\tilde{X}(f) = R(f)^{-1} \vec{d}(f, \hat{k}) : \vec{h} \quad (7)$$

$$R(f) = e^{i\pi fL/c} \left[ \text{sinc} \left( \frac{2\pi fL}{c} \right) \right]^{-1} \left( \frac{ic}{4\pi fL} \right) \xrightarrow{f \rightarrow 0} \left( \frac{ic}{4\pi fL} \right)$$

The difference from LWL is that the RA response tensor  $\vec{d}(f, \hat{k})$  depends on the Doppler parameters of the signal and introduces time-delays. After MLDC2, we found that much of the systematic error in the estimation of  $\mathcal{A}^\mu$  could be removed using only the RA scalar response  $R(f)$ , while still using the long-wavelength response tensor (referred to as “Partial Rigid Adiabatic” response [3]). For MLDC1b we implemented the Full Rigid Adiabatic response (7).

## Results

Challenge 1B.1.1 consists of three datasets (a,b,c), each containing one unknown white-dwarf binary (WDB) signal. Our MLDC1B entries used the full RA response, but we also searched the data sets using LWL and partial RA responses for comparison. In each case, the injected signal was recovered with accurate Doppler parameters, regardless of the TDI response used (Tab. 1).

$f$ (mHz)	$\Delta f$ (nHz)			$\phi_{\text{sky}}$ (mrad)			$\epsilon_\theta$			
	L	pR	R	L	pR	R	L	pR	R	
a	1.1	-2.4	-2.4	-2.4	104.5	104.5	104.5	1.3	1.3	1.3
b	2.9	0.9	0.9	0.9	56.0	56.0	56.5	0.5	0.5	0.7
c	9.9	1.8	1.8	1.8	30.8	30.8	26.6	1.5	1.5	1.2

**Table 1:** Doppler recovery in Challenge 1B.1.1a-c using rigid adiabatic (R), partial RA (pR) and long-wavelength (L) responses. Shown are the errors  $\Delta f$  in frequency, the sky angle  $\phi_{\text{sky}}$  between injected and recovered signals, and a metric error estimate  $\epsilon_\theta = \frac{1}{3} m |\mathcal{A}_{\text{key}}|^2$  (with expectation  $E[\epsilon_\theta] = 1$  in Gaussian noise).

On the other hand, the amplitude parameters  $\mathcal{A}^\mu$  are recovered significantly more accurately at higher frequencies using the full RA response rather than LWL (Fig. 3).

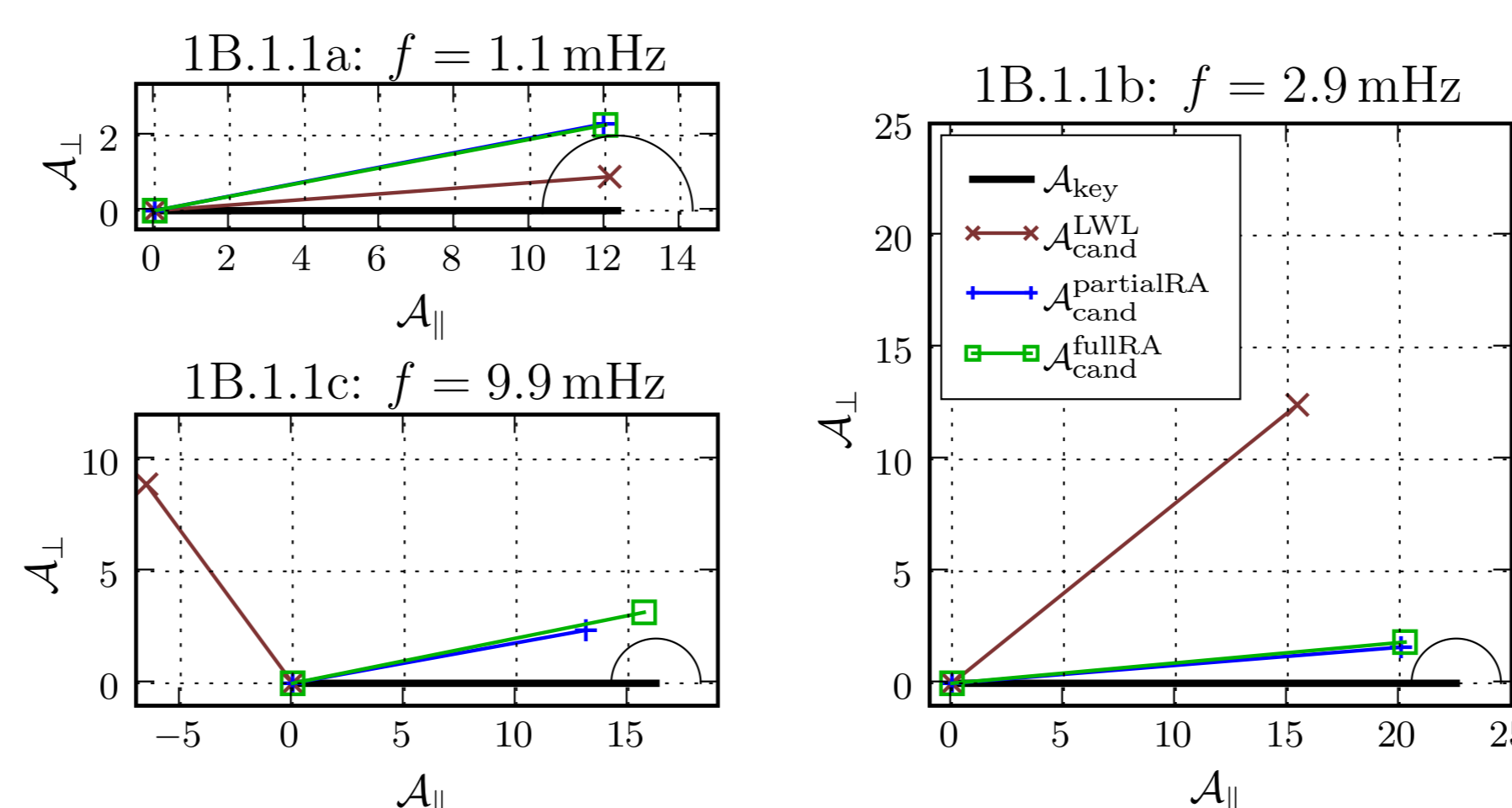


**Figure 3:** Amplitude parameter recovery in Challenge 1B.1.1. The black line is the injected amplitude 4-vector  $\mathcal{A}_{\text{key}}$ . Each recovered candidate 4-vector  $\mathcal{A}_{\text{cand}}$  is shown, with its components along and normal to  $\mathcal{A}_{\text{key}}$  using the metric  $\mathcal{M}_{\mu\nu}$ . The semicircle at the end of  $\mathcal{A}_{\text{key}}$  corresponds to a  $1\sigma$  deviation in Gaussian noise.

Challenge 1B.1.2 had 25 “verification binaries” with known Doppler parameters, but unknown amplitude parameters  $\mathcal{A}^\mu$ . Fig. 4 shows the amplitude recovery in this challenge and illustrates the improvement due to the full RA response.

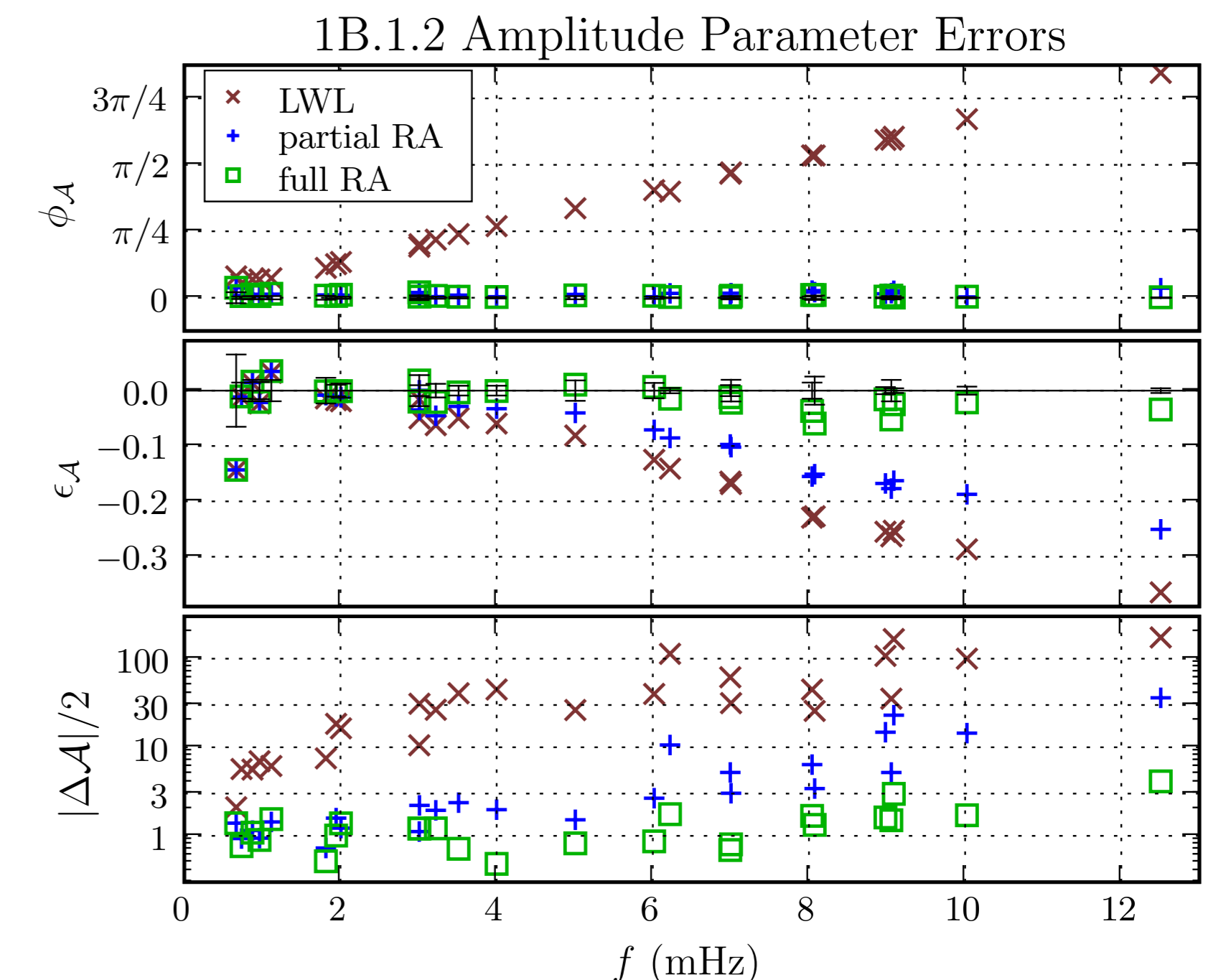


**Figure 4:** Amplitude parameter errors in Challenge 1B.1.2. Shown are the angle  $\phi_{\mathcal{A}}$  between the 4-vectors  $\mathcal{A}_{\text{cand}}$  and  $\mathcal{A}_{\text{key}}$ , the relative difference in “SNR”  $\epsilon_{\mathcal{A}} = \frac{|\mathcal{A}_{\text{cand}}|^2 - |\mathcal{A}_{\text{key}}|^2}{2|\mathcal{A}_{\text{key}}|^2}$ , and the “distance”  $|\Delta \mathcal{A}|$  between the two amplitude vectors. We see that the LWL results have a large systematic offset in  $\phi_{\mathcal{A}}$  and that the full RA results are considerably better than partial RA and LWL in recovering the length of  $\mathcal{A}_{\text{key}}$ .

Challenges 1B.1.3-5 were supposed to contain multiple binaries, increasingly crowded in Doppler space. Unfortunately, 1B.1.3 was generated with no detectable signals, as all had  $|\mathcal{A}_{\text{key}}| < 0.4$ . To check performance for resolvable, detectable binaries, we consider both MLDC1B and the earlier MLDC1, (“MLDC1A”), see Table 2.

Challenge	Found		Missed				False	
	1A	1B	$ \mathcal{A}_{\text{key}}  > 40$	1A	1B	$ \mathcal{A}_{\text{key}}  < 40$	1A	1B
1.1.3	15	0	2	0	3	20	4	0
1.1.4	18	11	23	23	4	18	6	2
1.1.5	3	3	30	28	0	13	0	0

**Table 2:** Signals found, signals missed, and false alarms in Challenges 1A.1.3-5 and 1B.1.3-5. We divided the missed signals into those with  $|\mathcal{A}_{\text{key}}| > 40$ , which should in principle be detectable with our current pipeline settings, and those with  $|\mathcal{A}_{\text{key}}| < 40$ , which are likely to be too weak to pass our detection threshold.

The corresponding Doppler parameter recovery for 1A.1.3 is shown in Fig. 5.

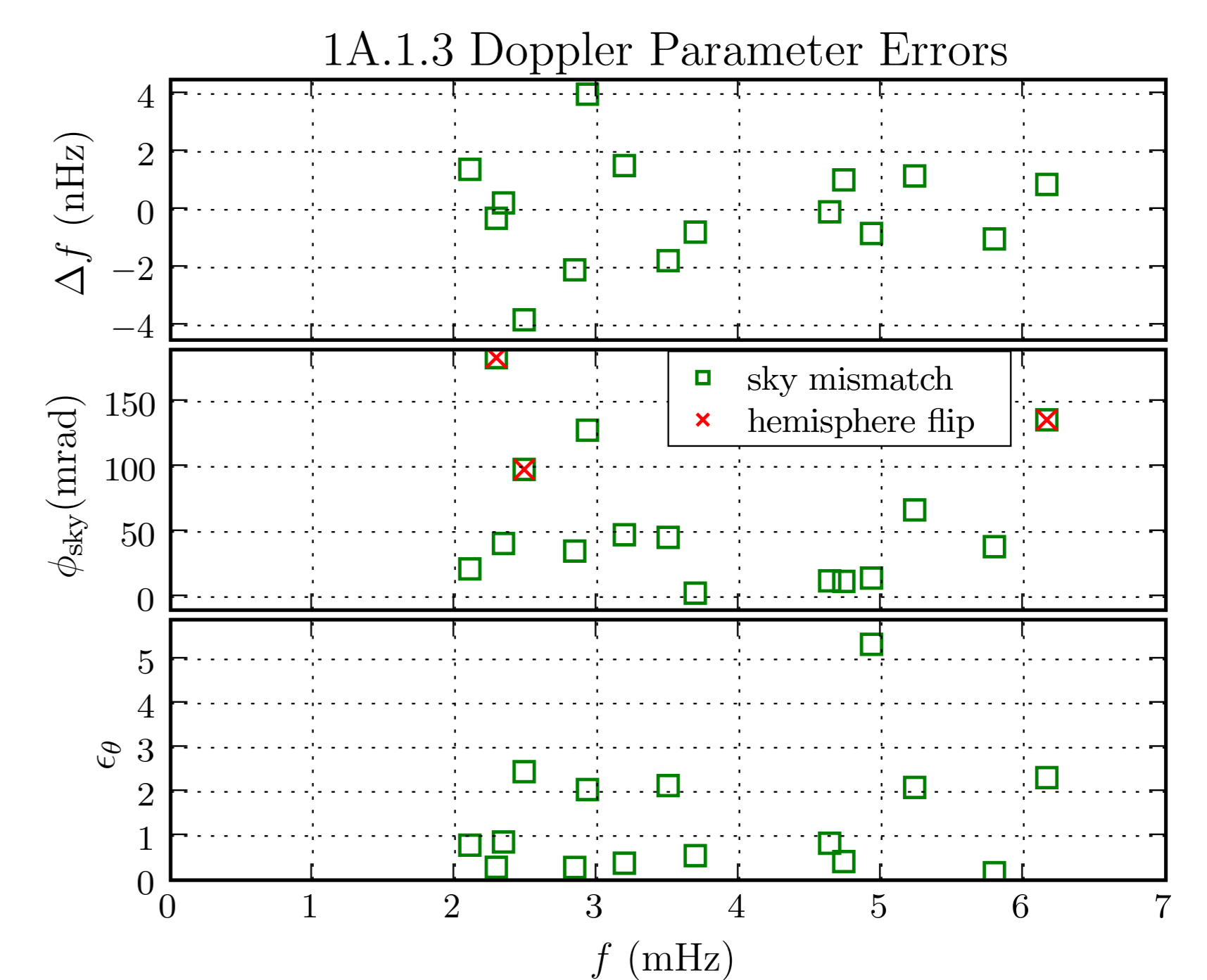


**Figure 5:** Doppler parameter recovery in 1A.1.3. The quantities plotted are defined in Table 1

## Summary

We searched for periodic signals from white dwarf binaries in MLDC1B, using an  $\mathcal{F}$ -statistic template bank. Coincidence between  $X, Y, Z$  TDI variables was used to distinguish primary from secondary maxima. The inclusion of the full rigid adiabatic response allowed amplitude as well as Doppler parameters to be accurately recovered.

## References

- [1] Prix & Whelan CQG24, S565 (2007)
- [2] Prix & Whelan, LIGO-G070462-00-Z
- [3] Whelan, LIGO-G070778-00-Z
- [4] Rubbo, Cornish & Pujade, PRD69, 082003 (2004)